



Cite this: *RSC Adv.*, 2024, **14**, 16228

## A novel nerol-segmented waterborne polyurethane coating for the prevention of dental erosion

Peipei Huang,<sup>ac</sup> Qiongfang Nie,<sup>b</sup> Yu Tang,<sup>b</sup> Shunshun Chen,<sup>b</sup> Kaiyuan He,<sup>b</sup> Mingguo Cao<sup>\*ac</sup> and Zefeng Wang 

Dental erosion is a common problem in dentistry, and it refers to the chronic pathological loss of dental hard tissues due to nonbacterially produced acids, primarily caused by the exposure of teeth to exogenous acids. Dietary factors play a pivotal part in the pathogenesis of dental erosion, with a high intake of acidic beverages leading to an increased prevalence of dental erosion in adolescents. Fluoride is mainly used in clinical practice to prevent dental erosion. However, long-term fluoride intake may lead to chronic fluorosis symptoms caused by fluoride overdose. Nano-coatings on dental surfaces have become a popular area of research in dental materials in recent years. The objective of this study was to develop a novel nerol-segmented waterborne polyurethane nano-coating to protect teeth from direct contact with an acidic environment and to provide a safe, effective method for preventing dental acid erosion.

Received 6th March 2024  
Accepted 10th May 2024

DOI: 10.1039/d4ra01744g  
[rsc.li/rsc-advances](http://rsc.li/rsc-advances)

## 1 Introduction

Dental erosion is the irreversible loss of tooth hard tissue. It is mainly caused by nonbacterial exogenous acids, which the teeth may come into contact with through the ingestion of acidic foods, beverages, or medications, as well as through occupational acid exposure.<sup>1</sup> In everyday life, dental erosion caused by long-term high intake of carbonated beverages is extremely common, and this is commonly known as “cola teeth”. Acid-eroded teeth initially show dentinal sensitivity, and this later progresses to significant defects that can cause aesthetic problems. Pulp exposure can occur in advanced stages.<sup>2</sup> Current preventive strategies for dental erosion include oral-health education and topical application of antiacid erosion agents. The most common of these is fluoride, which prevents tooth demineralisation and promotes surface remineralisation in an acidic environment.<sup>3</sup> Topical application of fluoride is safe, but excessive fluoride intake over a long period of time can lead to symptoms of chronic fluorosis such as dental fluorosis, osteofluorosis, loss of muscle strength and low haemoglobin.<sup>4</sup> Therefore, new techniques in contemporary dentistry are necessary to provide more effective strategies.

Nanotechnology is currently being used in various areas of dentistry, including preventive dentistry, restorative dentistry, endodontics and periodontics. The surface of the tooth has

a unique morphology with pits and fissures, and nanoparticles can enter these gaps more easily than other materials. Nanomaterials are generally classified as organic nanomaterials, inorganic nanomaterials and carbon-based nanomaterials.<sup>5,6</sup> Polymeric materials (e.g., polyethylene, polypropylene, polymethyl methacrylate, polyurethane, poly(vinyl alcohol), poly(lactic acid) and poly(caprolactone)) are widely used in the biomedical field owing to their excellent mechanical properties, biocompatibility and biodegradability, and they have better film-forming properties than inorganic nanomaterials.<sup>7</sup> Polymer films have been used in numerous studies to protect teeth from acid erosion by preventing direct contact with the acidic environment of the mouth. da Silva Ávila *et al.*<sup>8</sup> investigated the effectiveness of the acrylic polymer kapop in preventing or controlling acid erosion of tooth enamel and its protective effect against tooth demineralisation. Dental polymers must meet high standards for aesthetics, toughness, and biocompatibility. They should not compromise the appearance of teeth, and they should withstand occlusal and frictional forces. However, acrylic polymers are known for their poor mechanical strength.

Polyurethane is a polymer that is composed of alternating rigid and flexible segments that are joined together to enhance flexibility, toughness, and scratch resistance.<sup>9</sup> The depletion of petroleum-based materials and environmental concerns have increased awareness of the importance of using bio-based materials in recent years. As a result, researchers have begun to synthesise bio-based waterborne polyurethanes (WPUs) using water as the dispersion medium and bio-based materials instead of petroleum-based materials.<sup>10-13</sup> Carboxylic acid-containing chain extenders, which introduce carboxyl groups to make the molecular chain hydrophilic, are frequently used in

<sup>a</sup>College of Stomatology, Hangzhou Normal University, Hangzhou 310000, China

<sup>b</sup>Department of Chemistry, Lishui University, Lishui 323000, China. E-mail: cmg@lzu.edu.cn; shangk72@163.com

<sup>c</sup>Department of Medicine, Lishui University, Lishui 323000, China

<sup>d</sup>R&D Center of Green Manufacturing New Materials and Technology of Synthetic Leather, Sichuan University, Lishui 323000, China



waterborne polyurethanes to improve dispersion in the aqueous phase. Further, polymers containing carboxyl groups can adhere to enamel and dentin surfaces by forming ionic bonds with calcium from hydroxyapatite.<sup>14</sup> In addition to environmental friendliness and biodegradability, bio-based materials are antimicrobial, anti-inflammatory, anti-oxidant, low in cytotoxicity and biocompatible,<sup>15–19</sup> and their incorporation can improve the bioactivity of waterborne polyurethanes. Therefore, bio-based waterborne polyurethanes show promise in dental coatings research.

Nerol (*cis*-2,6-dimethyl-2,6-octadien-8-ol) is a monoterpenoid compound found in medicinal plants such as *Lippia* spp. and *Balsamina*. It exhibits antimicrobial, anti-oxidant, and antiviral properties.<sup>20</sup> The physico-mechanical properties of waterborne polyurethane decrease as the number of hydroxyl groups increases, which is attributed to a decrease in the content of hard segments.<sup>21,22</sup> The biological activity of traditional natural bio-based materials, such as lignin and castor oil,<sup>23,24</sup> is relatively low, and some bio-based polyurethane materials are introduced by physical blending of bioactive ingredients with poor stability. In contrast, nerol is more stable in the system for the hydroxyl active functional group, which can be bonded with isocyanato group. Meanwhile, its antibacterial and anti-inflammatory can have a good therapeutic effect in the biomedical field of gingivitis, dental acidosis and other symptoms. In addition, as a protective coating, the appropriate hydrophobicity is conducive to shielding the corrosion of water-soluble acids. Nerol is beneficial to the application of the protective coating for dental acidosis for its good hydrophobicity.

This study involved the preparation of four groups of novel nanoscale waterborne polyurethanes using PEBA-1000, IPDI, DMBA, TEA, and nerol at concentrations of 0%, 2%, 4% and 8%. A series of characterisations, such as particle size, zeta potential, transparency, scanning electron microscopy, thermal properties, and contact angle, were tested to compare the physicochemical properties of every group of waterborne polyurethanes. Additionally, we analysed the biological properties of every group of waterborne polyurethanes through simulations of an acid attack, anti-protein adhesion, and anti-inflammation experiments. After analysing the experimental data, we found that the waterborne polyurethane containing 2% nerol had a better overall performance, not only effectively avoiding direct contact between the teeth and the acidic environment, but also exhibiting good physicochemical properties and other biological properties.

## 2 Materials and methods

### 2.1 Materials

2,2-Dihydroxymethylbutyric acid (DMBA, 98%), isophorone diisocyanate (IPDI), nerol (97%), triethylamine (TEA), tetrahydrofuran (THF, 99%), chloroform-d (CDCl<sub>3</sub>, 99.8%), acetic acid (99.5%), toluidine blue (TB), sodium hydroxide (NaOH, 95%), and sodium dodecyl sulfate (SDS, 99.5%) were purchased from Macklin Chemical Reagent Co. Ltd, Shanghai, China. Deionised water is prepared in the laboratory. PEBA (Mn = 1000 g mol<sup>-1</sup>)

and acetone were kindly gifted by Zhejiang Demei Boda Polymer Material Co. Ltd, Zhejiang, China.

### 2.2 Synthesis of waterborne polyurethanes

PEBA and IPDI were placed in a three-necked flask equipped with a mechanical stirrer and reacted at 90 °C for 2 h. The mixture was then cooled to 75 °C and DMBA was added to continue the reaction for 2 h. At this point, there were still unreacted isocyanate groups in the reaction system as determined by the di-*n*-butylamine method as shown in Table 1.<sup>25</sup> The mixture was cooled to 60 °C and nerol was added to react the mixture for 2 h to consume the –NCO groups sufficiently, and then triethylamine was added to neutralise the mixture for 15 min. Acetone was then added to adjust the viscosity of the prepolymer. Finally, 150 ml of deionised water was added and emulsified for 10 min at a stirring speed of 2000 rpm to obtain a WPU-N emulsion with a certain solid content. The formulations used are shown in Table 2. WPU-N0% means no addition of nerol, WPU-N2% means the addition of nerol is 2% of the sum of the mass of IPDI and PEBA, and WPU-N4% and WPU-N8% have the same meaning. The above synthetic route is shown in Fig. 1.

### 2.3 Characterisations

**2.3.1 Physical and chemical characterization of WPUs.** The infrared absorption spectra of the WPU films was tested in the 4000–500 cm<sup>-1</sup> band using a Fourier transform infrared spectrometer (Nicolet IS10, Nicolet, USA). Each film sample was dissolved in THF and the molecular weight of WPU films was determined by gel permeation chromatograph (Waters 1515, America). For <sup>1</sup>H NMR analysis, 10 mg of the sample was weighed and dissolved in 0.5 ml of CDCl<sub>3</sub>, recorded on a NMR spectrometer (Bruker Avance 300, Germany). Particle size and zeta potential of the WPU emulsions were determined using a nanoparticle size and zeta potential meter (Zetasizer Nano ZS, Malvern, UK) and the emulsions were appropriately diluted with deionised water prior to testing. The thermal decomposition of the WPU films was tested from 35 °C to 600 °C using a simultaneous thermal analyser (STA 449 F5 Jupiter, NETZSCH, Germany) under a nitrogen atmosphere at a ramp rate of 10 °C min<sup>-1</sup>. Differential-scanning calorimetry scans were performed using a differential-scanning calorimeter (DSC 214 Polyma, NETZSCH, Germany) in a nitrogen atmosphere from –90 °C to 200 °C at a ramp rate of 10 °C min<sup>-1</sup>. The transmittance and haze of the WPU films were tested using a transmittance/haze tester (WGT-S, INESA Physico-Optical Instrument Co. Ltd, Shanghai, China). The water-contact angle of the WPU films was measured using a contact-angle tester (JY-PHC, Chengde Jinhe Instrument Manufacturing Co. Ltd, China). SEM images of the WPU coatings were obtained using a scanning electron microscope (SU8010, HITACHI, Japan), and the samples were sprayed with gold to improve conductivity before testing. The number of carboxyl groups on the surface of WPU films was determined using spectroscopic UV-vis toluidine blue (TB) titration. WPU films (formed on 2.5 cm × 2.5 cm slides) were acidified in 50% acetic acid and then rinsed with



**Table 1** Residual NCO% before and after adding nerol

	First determination of NCO% (IPDI + PEBA + DMBA)	Second determination of NCO% (after adding nerol)	Difference
WPU-N2%	4.71	3.46	1.25
WPU-N4%	4.53	3.19	1.34
WPU-N8%	4.74	3.93	1.44

**Table 2** Formulation of waterborne polyurethanes (mmol)

Sample	IPDI	PEBA	DMBA	Nerol	TEA
WPU-N0%	108.0	52.1	19.9	0.0	19.9
WPU-N2%	108.0	47.4	19.9	9.3	19.9
WPU-N4%	108.0	43.4	19.9	17.5	19.9
WPU-N8%	108.0	37.3	19.9	31.8	19.9

deionised water. The acidified WPU films were incubated in alkaline aqueous solution (5 mM TB in 0.1 mM NaOH) for 2 h and washed with 0.1 mM NaOH solution to remove the non-complexed TB. The adequately washed WPU films were immersed in 10 ml of 50% acetic acid for 1 h. A UV-vis

spectrophotometer (Cary 60, Agilent, USA) was used to measure the absorbance of TB in an acidic solution at 635 nm. This study used HA disc (purchased from Shanghai Aladdin Biochemical Technology Co., Ltd) instead of tooth to test the adhesion of WPU coating to tooth, since the main component of dental hard tissue is hydroxyapatite. The bond strength was measured using a nano-indenter (Anton-Paar NHT + MCT, Switzerland), and the bond strength was evaluated by the critical load of coating damage.

**2.3.2 Cola-erosion experiment.** In this study, dentinally intact premolar teeth extracted for orthodontic reasons at the Department of Dentistry, Lishui College Hospital were used and stored in saline at 4 °C after gentle removal of periodontal soft tissue with a scalpel. (This study was approved by the Medical Ethics Committee of the Medical College of Lishui University, No. 2023YR0041.) The WPU emulsions were applied to the crown portion of the teeth using a small dental brush and dried naturally to form the film. The isolated teeth of each group were immersed in cola for 3 days and replaced with new fresh cola every 24 h. Photographs were taken to record the colour change of the crowns.

**2.3.3 Anti-protein adhesion test.** Drops of WPU emulsions were placed on 1 cm × 1 cm slides to form the films, and a blank slide was used as the control. The samples were placed in 0.5 mg mL<sup>-1</sup> bovine serum albumin (purchased from Macklin

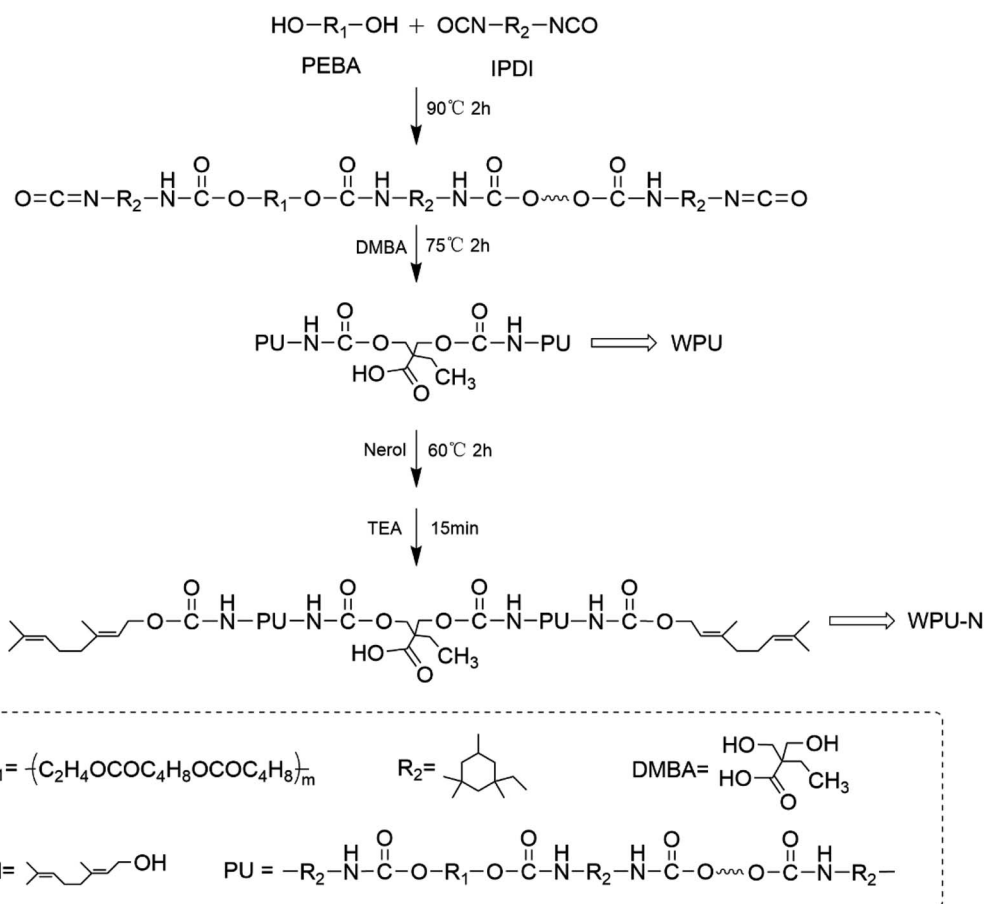


Fig. 1 Synthesis route of nerol-segmented waterborne polyurethane

Chemical Reagent Co. Ltd) solution at 37 °C for 1 h. The samples were washed three times with deionised water and then transferred to 1 wt% SDS solution and ultrasonicated for 10 min. After that, the samples were analysed using a BCA Protein Concentration Determination Kit (Beyotime Biotechnology Co. Ltd, China) and a UV-vis spectrophotometer (at 562 nm) to measure the absorbance. The amount of BSA solution and SDS solution added to each group was the same.

**2.3.4 Anti-inflammatory activity.** RAW264.7 macrophages in logarithmic growth phase were inoculated in 96-well plates at a density of  $2 \times 10^4$ /ml and cultured at 37 °C and 5% CO<sub>2</sub> under humid conditions for 24 h, and then LPS (500 ng ml<sup>-1</sup>) was added for 4 h to induce cellular inflammation. No material was added to the control group, 3  $\mu$ L of WPU emulsions with different nerol content were added to the experimental groups, and dexamethasone aqueous solution (900  $\mu$ g ml<sup>-1</sup>) was added to the positive control group. Each group was incubated for 24 h. The medium in the wells was aspirated and centrifuged, and the supernatant was taken to detect inflammatory factors, using a mouse interleukin 6 (IL-6) ELISA kit (Jingmei Biotechnology Co. Ltd, China).

### 3 Results and discussion

#### 3.1 Chemical structure of WPU films

Fig. 2 shows the FT-IR spectra of the four WPU films with very similar results. The stretching vibrations and bending vibrations of N-H at 3368 cm<sup>-1</sup> and 1526 cm<sup>-1</sup>, respectively. The peak at 2950 cm<sup>-1</sup> is attributed to stretching vibrations of C-H. The characteristic peaks at 1724 cm<sup>-1</sup>, 1233 cm<sup>-1</sup> and 1136 cm<sup>-1</sup> are owing to the stretching vibrations of C=O, C-N and C-O, respectively.<sup>26,27</sup> In summary, the polymer contains carbamate group in the main chain, which is the characteristic unit of polyurethane.

According to the GPC curve, the M<sub>w</sub> (molecular weight) of WPU gradually decreases with the adjustment of the addition amount of PEBA and nerol, and WPU-N8% is the smallest (Fig. 3). The possible reasons are as follows: the nerol content of WPU-N8% is the highest, and nerol plays an end-sealing role in the polymerization chain, preventing the continued extension of the polymer chain. Therefore, the M<sub>w</sub> of WPU decreased with the addition of nerol. In addition, compared with WPU-N0%, the curve peak width of the other three groups is narrower, indicating better homogeneity of the polymer, which is conducive to reducing the difference between product batches during production.

Additionally, <sup>1</sup>H-NMR spectroscopy of WPUs were detected, respectively. Compared to the original WPU, WPU-N2%, WPU-N4% and WPU-N8% show significant new peaks, indicating its successful modification. For example, as shown in Fig. 4, two new resonances at 6.0–5.0 ppm (a) emerge for WPU-N2%, WPU-N4% and WPU-N8%, which are ascribed to the two –C=C–H groups. Furthermore, new signals at 2.5–2.0 ppm (b) and 5.0–4.5 ppm (c) are assigned to methylene groups of nerol. All these remarkable chemical shifts further indicate the successful modification. We also measured the carbon spectrum at the same time, but due to the reduced content, no significant nuclear magnetic peak was detected.

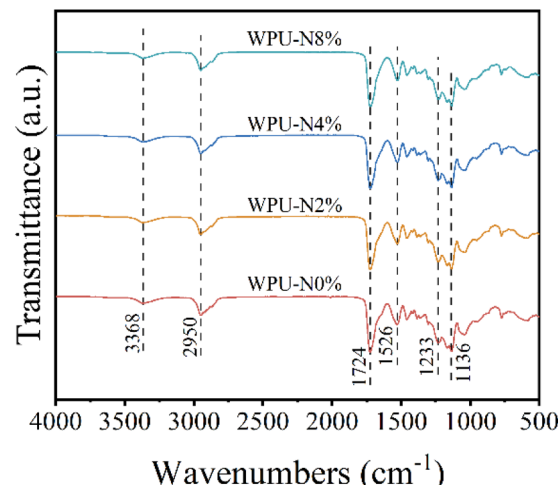


Fig. 2 FT-IR spectra of WPU films.

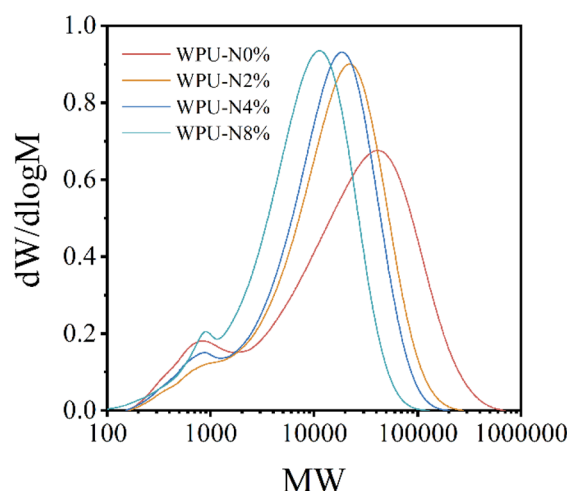


Fig. 3 Gel permeation chromatography analysis of WPUs.

#### 3.2 Particle size and zeta potential of WPU emulsions

The toxicity of nanoparticles is closely related to their physical properties, such as size, shape and surface charge.<sup>28</sup> In addition, particle size and zeta potential are important parameters for assessing the storage stability of waterborne polyurethanes.<sup>29</sup> Therefore, we characterised the particle size (a–d) and zeta potential (e) of the waterborne polyurethane emulsions prepared in this study, and the results are shown in Fig. 5. It has been shown that 10 nm nanoparticles administered intravenously to rats the distribution of nanoparticles in vital organs such as the heart, lungs and brain, while most 50–250 nm nanoparticles are found in the liver, spleen, and blood and are metabolized and eliminated from the body.<sup>30</sup> The percentage of nanoparticles larger than 50 nm in all four of the groups of WPU emulsions in this study exceeded 80%, with WPU-N2% reaching 95%. The average particle sizes of WPU-N0%, WPU-N2%, WPU-N4%, and WPU-N8% were 83.55, 83.55, 78.37, and 158.01 nm, respectively. The particle size and distribution width of the



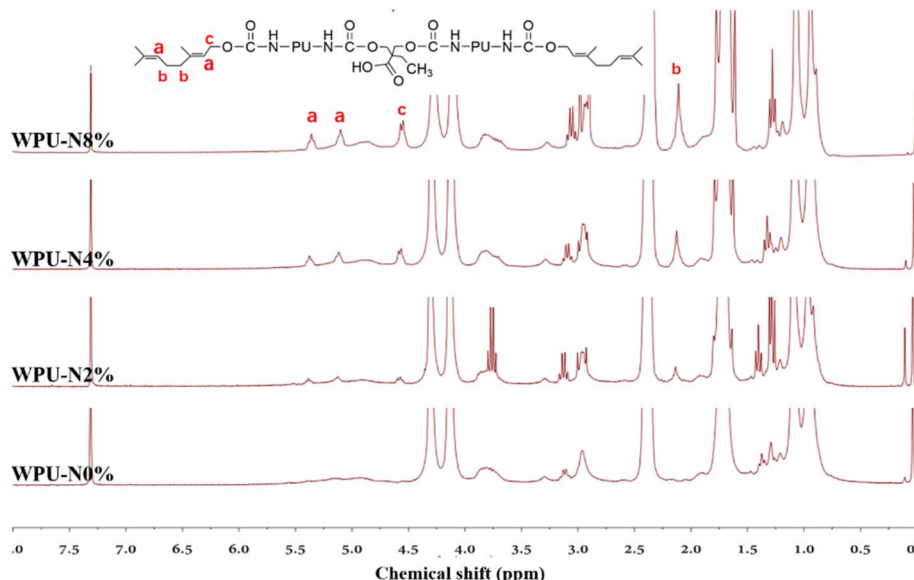


Fig. 4  $^1\text{H}$  NMR spectrum of WPU films.

WPU emulsion first decreased slightly and then increased with the addition of nerol. The hydrophobic segments are wrapped by the hydrophilic groups inside the nanoparticles when the nerol content is low, so hydrophobicity does not dominate and the particle size of the nanoparticles does not increase at this time. Nerol is hydrophobic,<sup>31</sup> and as the content of nerol increases, the hydrophilic carboxyl groups are unable to wrap all of the hydrophobic segments, thus resulting in an increase in the average particle size of the emulsion. Positively charged nanoparticles are more likely to enter the cell under electrostatic attraction because glycoproteins on the surface of the cell membrane are negatively charged.<sup>28</sup> After neutralisation with triethylamine, the zeta potentials of the WPU emulsions were still negative and the absolute values were all greater than 70 mV. In summary, in terms of particle size and charge, the WPU nanoparticles in this study may have relatively low toxicity. In contrast, the higher absolute value of the zeta potential indicates that the emulsion has good storage stability. As can be seen from the appearance graph (Fig. 5f-h), the emulsion was stable during storage without any obvious precipitation at the bottom. In addition, the emulsions had good fluidity without the wall-hanging phenomenon, which facilitated flow and diffusion on the uneven tooth surface.

### 3.3 Transparency and SEM morphology of WPU coatings

Most carbonated beverages contain pigments, and teeth are will be corroded at the same time that discolouration occurs, seriously affecting teeth aesthetics. This requires that the coating does not change the original colour of the teeth while protecting them, so being colourless and transparent is an important characteristic of the WPU coating. Transmittance and haze are important characterisations of transparent materials, and Fig. 6 shows the transmittance (a) and haze (b) of WPU coatings with different nerol contents. The transmittance of the WPU-N0%

coating was 87%, and the addition of nerol increased the transmittance of the WPU, while the other three groups had transmittances around 91%. In general, the higher the transmittance of a material, the lower the haze. The haze of the WPU-N0% coating was 12%, and the addition of nerol reduced the haze of the WPU coatings to almost 0%. Less haze means better gloss and transparency of the coating. As can be seen from the coating appearance graph (Fig. 6c and d), the WPU coatings in this study were colourless and transparent, but the surface of the WPU-N0% coating is wrinkled, while the surface of the WPU-N2% coating was smooth and flat. Fig. 6(e and f) shows the microscopic morphology of the WPU-N0% and WPU-N2% coatings that had been captured by SEM, and we can see more wrinkles on the surface of the WPU-N0% coating. Although wrinkles could also be seen on the surface of the WPU-N2% coating, they were reduced in number and finer. Surface roughness is an influential factor in oral bacterial adhesion,<sup>32</sup> and a smooth surface reduces bacterial adhesion. Additionally, the transparency of smooth, flat coatings can provide high transmittance since it does not impair light transmission.<sup>33</sup>

### 3.4 Thermal properties of WPUs

Compared with other coatings, dental coatings need to have good thermal stability owing to the special characteristics of the oral environment, which makes contact high-temperature food, so we tested the TG curves (a) and DTG curves (b) of the WPU coatings with different nerol contents. The results are shown in Fig. 7. The initial decomposition temperature, half-life temperature and maximum thermal decomposition temperature are given in Table 3. The decomposition temperature range of the WPU coatings was 250–450 °C, which is much higher than the temperature of the mouth and hot food. From the DTG curves, it can be seen that WPU-0% had two thermal decomposition phases, and that the thermal decomposition process of



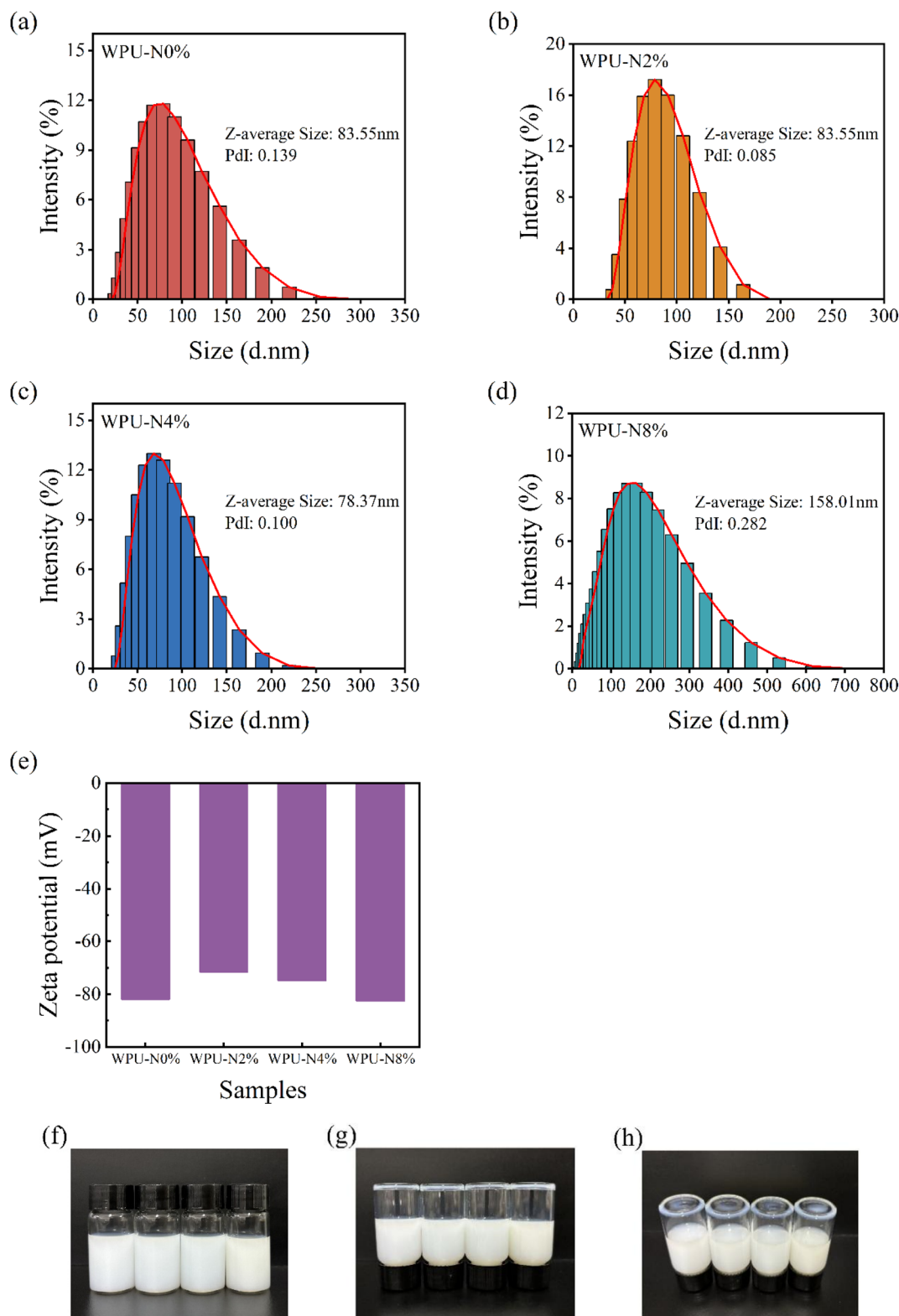


Fig. 5 (a-d) Particle size and distribution of WPU emulsions; (e) zeta potential of WPU emulsions; (f-h) appearance of WPU emulsions and from left to right are WPU-N0%, WPU-N2%, WPU-N4%, WPU-N8%.

WPU with the addition of nerol became more complicated with more than two thermal decomposition phases, which may be related to the free nerol. The thermal decomposition process of

WPU-4% was essentially similar to that of WPU-N0%, while WPU-2% and WPU-N8% showed a shift to the left, indicating a slight decrease in thermal stability. As the nerol content

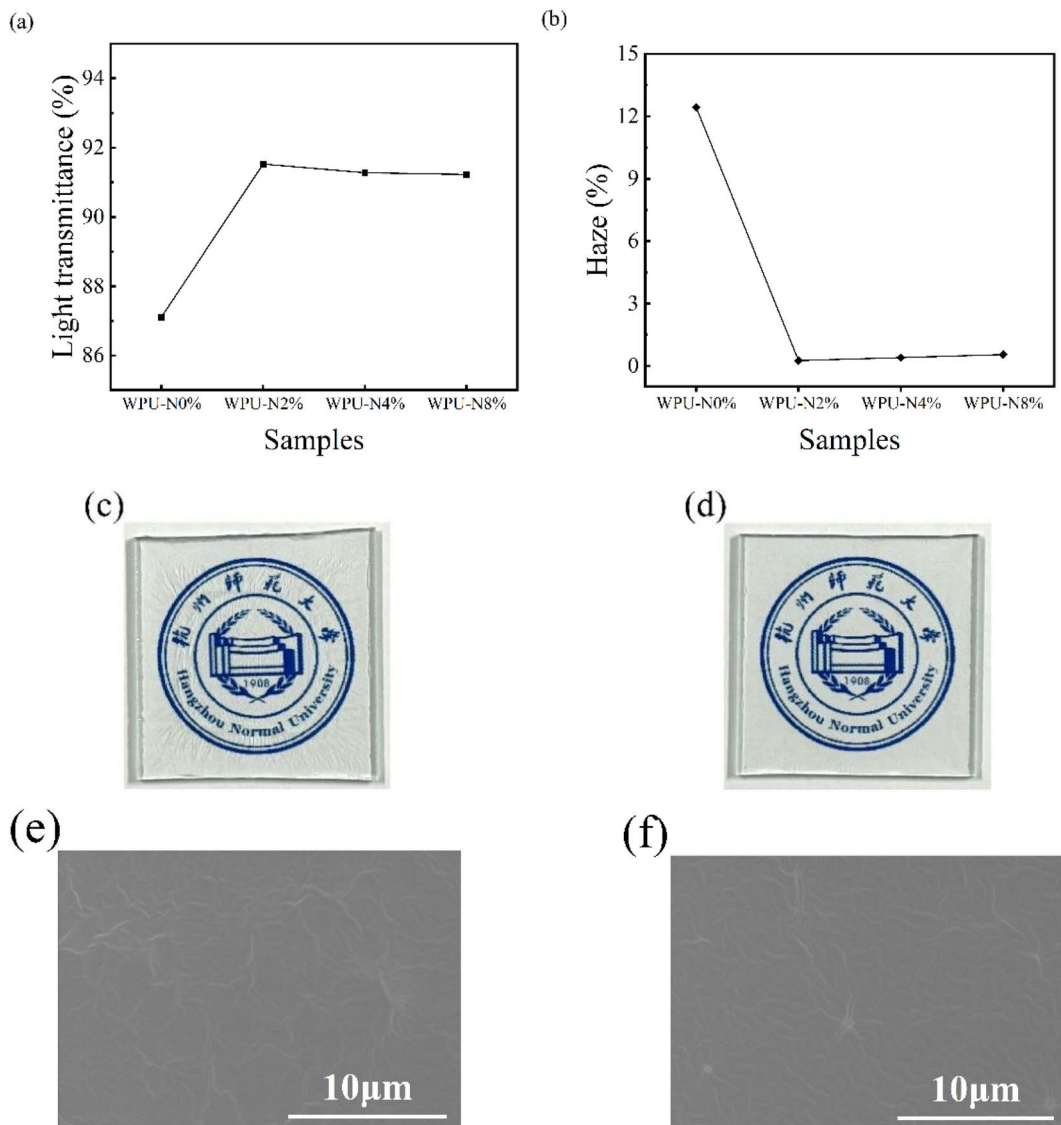


Fig. 6 Light transmittance (a) and haze (b) of WPU coatings; appearance of WPU-N0% coating (c) and WPU-N2% coating (d); SEM images of WPU-N0% coating (e) and WPU-N2% coating (f).

increased, the thermal stability of the WPU first worsened, then improved, and then worsened again. The  $-\text{NH}-$  of waterborne polyurethanes could form hydrogen bonds, most of which were formed with the carbon groups in the hard segments and a small proportion between the ether oxygens or ester carbonyls in the soft segments.<sup>34</sup> Owing to the large spatial site resistance of nerol, it is possible that when added in small quantities, the hydrogen bonds in waterborne polyurethanes will be broken, resulting in a slight decrease in thermal stability. When added in more quantities, they will clump by themselves and the part of the hydrogen bond that has clumped will be retained. However, if nerol is added, the bonds will begin to squeeze around and interfere with the hydrogen bond regions again, resulting in another decrease in thermal stability. Additionally, we measured the DSC curve of WPU-N8% (c), which showed that two glass-transition processes,  $T_{\text{g}_1}$  and  $T_{\text{g}_2}$ , were the glass transition temperatures of the soft and hard segments, respectively,

indicating that this waterborne polyurethane is a combination of soft and hard segments. Coatings that are too soft are prone to loss, while those that are too hard are prone to brittle fractures, so a combination of soft and hard is preferable.

### 3.5 Water contact angle of WPU coatings

We measured the water contact angle of the WPU coatings, and the results are shown in Fig. 8. The water contact angle of the WPU coating gradually increased with increasing nerol content. The length of the hydrocarbon group had a direct effect on the hydrophilicity of the molecule, with long-chain hydrocarbon groups usually being nonpolar and, therefore, hydrophobic. Nerol contains 10 carbon atoms and belongs to medium-chain alkanes, the addition of which improves the hydrophobicity of waterborne polyurethane coatings. Because acid is hydrophilic, it erodes the tooth using water as a medium, so the increased



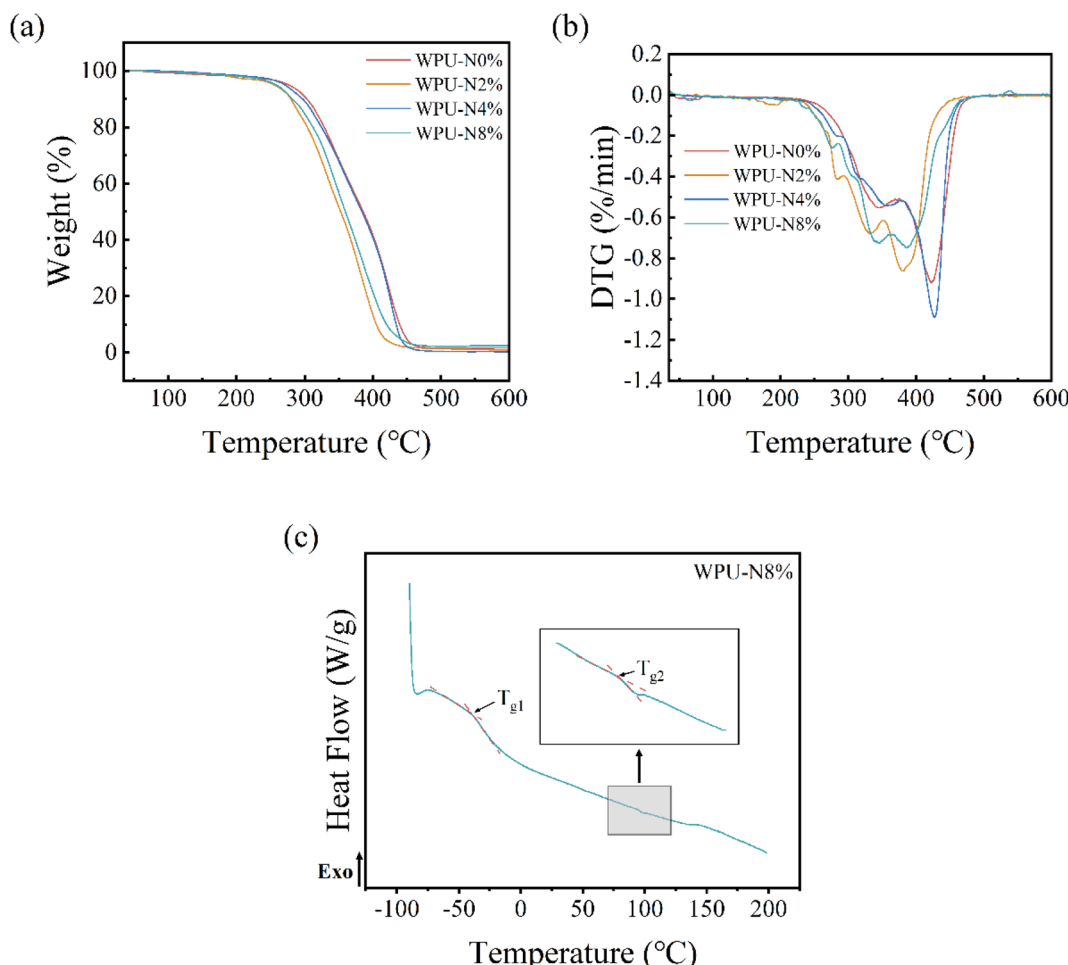


Fig. 7 TG curves (a) and DTG curves (b) of WPU coatings; (c) DSC curve of WPU-N8% coating.

Table 3 TGA data of WPU with different nerol content

Samples	$T_{5\%}$ (°C)	$T_{50\%}$ (°C)	$T_{\max}$ (°C)
WPU-N0%	276.5	385.9	422.9
WPU-N2%	255.7	353.0	379.8
WPU-N4%	270.9	384.1	427.2
WPU-N8%	258.0	359.8	384.9

hydrophobicity of the coating facilitates protection of the tooth from the acid, with the carboxyl moiety of the waterborne polyurethane binding to the calcium on the tooth surface and the hydrophobic segments provided by nerol forming a hydrophobic shell.

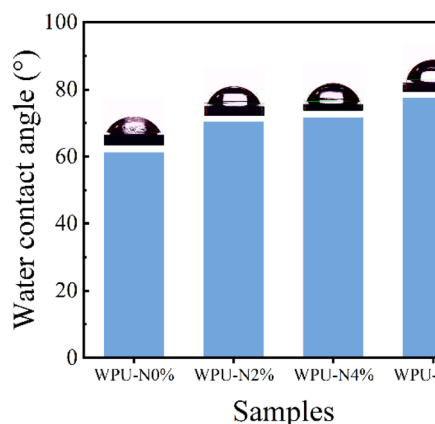


Fig. 8 Contact angle of WPU coatings with different nerol contents.

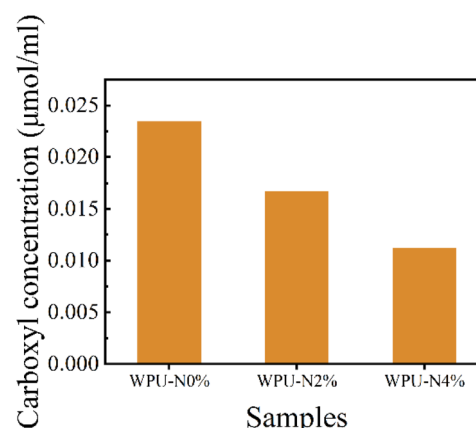


Fig. 9 Carboxylic group concentration on the surface of WPU-N0%, WPU-N2% and WPU-N4% coating (2.5 cm × 2.5 cm).

### 3.6 Carboxyl content of WPU coatings

Spectroscopic UV-vis toluidine blue titration is based on the pH-dependent adsorption/desorption of blue and positively charged TB ions on negatively charged surfaces, which adsorb in alkaline media and desorb in acidic media.<sup>35</sup> We used this method to determine the carboxylate concentration on the surface of the 2.5 cm × 2.5 cm WPU coating, assuming that TB would react with -COOH on the coating surface in a 1 : 1 ratio. The results are shown in Fig. 9. This experiment demonstrated that the surface of the WPU coatings in this study was carboxylated, and that the carboxyl group bound to the calcium ions on the tooth surface to enhance the adhesion of the coating, which facilitated the coating to provide a stable protective

effect. As the nerol content increased, the amount of carboxyl groups on the surface of the WPU coating gradually decreased. The WPU-N8% coating was not tested in this experiment owing to its tendency to swell after prolonged immersion in the solution, which caused film loss from the edge of the slide. Because the amount of IPDI and DMBA added to each group of WPU was the same, and the molar ratio of isocyanate groups to hydroxyl groups of the input raw materials was all 1.5 : 1, the amount of PEBA added decreased as the amount of nerol added increased. The WPU's main chain was formed through the reaction of IPDI and PEBA, and the amide group in the main chain depended on the amount of PEBA. As the amide group can be hydrolysed in water to produce carboxyl groups, the carboxyl group content decreased with the addition of nerol.

Table 4 Appearance of teeth exposed to cola

	Initial	Coated	Exposure to cola for 24 h	Exposure to cola for 48 h	Exposure to cola for 72 h
Uncoated		—			
WUP-N0%					
WUP-N2%					
WUP-N4%					
WUP-N8%					



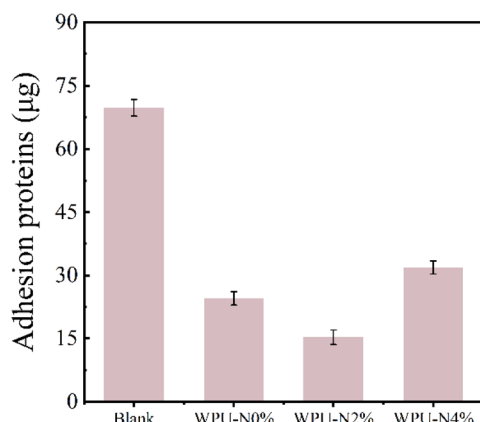


Fig. 10 Amount of bovine serum albumin adhering to the surface of WPU-N0%, WPU-N2% and WPU-N4% coating (1 cm × 1 cm).

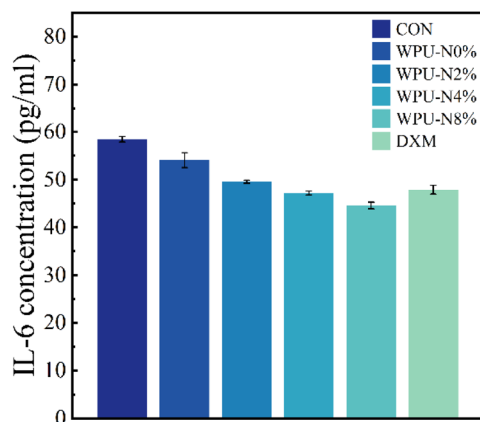


Fig. 11 WPUs with different nerol content, CA and DXM after 24 h co-culture with inflammatory induced macrophages and the analysis of IL-6 concentration by ELISA.

### 3.7 Cola erosion experiment

Table 4 shows the colour changes of isolated teeth in each group after 24, 48 and 72 h of immersion in cola. After the application of the coating, there was no significant change in the colour or gloss of the teeth, thus indicating that the WPU coatings in this study do not affect the aesthetics of the teeth. After 24 h of immersion, the enamel surface of uncoated teeth exhibited staining, which became more severe in terms of depth and area with increasing immersion time. None of the four coating groups exhibited significant discolouration on the tooth surface after 24 h of immersion. Moreover, WPU-N0% and WPU-N2% did not show any significant discolouration even after 72 h, indicating the effectiveness of the coatings in preventing direct contact of teeth with the acidic environment. However, from 48 h onwards, the WPU-N4% and WPU-N8% coating groups exhibited spotty colouration, indicating a loss of coating at the colouration site. This may be attributed to the softer coatings and lower carboxyl-group content in these two groups.

### 3.8 Anti-protein adhesion properties of WPU coatings

Fig. 10 displays the results of the bovine serum albumin adhesion experiments for WPU-N0%, WPU-N2% and WPU-N4% coating. The WPU-N8% coating test was cancelled for the same reason as the carboxyl content experiment. In all three of the groups, the amount of BSA adhering to the surface of the WPU coating was significantly reduced compared with the blank slides. The amount of BSA adhering to the surface of the WPU coatings first decreased and then increased as the nerol content increased. At a high pH, BSA carries a negative charge.<sup>36</sup> The zeta potential result reveals that the WPUs were also negatively charged. Therefore, the amount of protein adhering to the surface of WPU-N0% and WPU-N2% was reduced. In contrast, the protein adhering to the WPU-N4% surface slightly increased compared with the previous two groups. This may be because of the high content of nerol, which increases the viscosity of the coating. Saliva proteins consist mainly of mucins, which are classified into two types: high-molecular-weight mucin type (MG1) and low-molecular-weight mucin type (MG2). The primary role of MG1 is to adhere to dentine and mucosal surfaces and contribute to membrane formation, typically carrying a high negative charge.<sup>37</sup> Therefore, the WPU-N coating protects teeth from acid erosion and resists the adhesion of MG1, inhibiting the formation of acquired film and reducing the incidence of caries. Note that the amount of nerol should be appropriate.

### 3.9 Anti-inflammatory properties of WPUs

Coatings applied to tooth surfaces inevitably come into contact with the gingiva and oral mucosa. To prevent inflammatory-type complications such as gingivitis caused by the WPU coatings in this study, we performed anti-inflammatory experiments on them. Fig. 11 shows the anti-inflammatory results of WPU-N0%, WPU-N2%, WPU-N4%, WPU-N8% and dexamethasone (DXM). The concentration of IL-6 expressed was reduced in all of the WPU groups compared with the inflammation-induced group without any added material. Further, the concentration of IL-6 decreased progressively with the increase of nerol content. The anti-inflammatory effects of WPU-N2% and WPU-

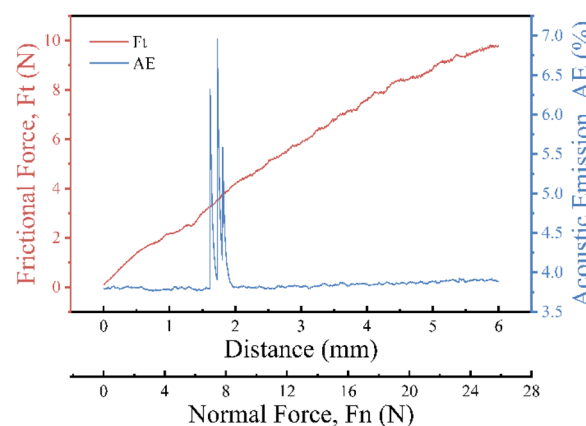


Fig. 12 Scratch test result of WPU-N2% coating.



N4% were comparable with that of DXM, and the anti-inflammatory effect of WPU-N8% was even slightly better than that of DXM. Thus, it is evident that the WPU in this study not only does not cause inflammation, but it also has an anti-inflammatory effect. In addition, WPU-N may be applied in the treatment of gingivitis or periodontitis, but this notion needs to be further investigated.

### 3.10 Bond strength of WPU-N2% coating to hydroxyapatite

Based on the results of the previous characterization, WPU-N2% showed the best overall performance, so we used it to test adhesion to teeth.<sup>38</sup> Fig. 12 shows the scratch test results of the WPU-N2% coating. It shows that the acoustic emission changes greatly at 6.71 N, indicating that the coating is scratched at this time, so the critical load is 6.71 N. Studies have shown that the average brush force of the toothbrush during daily brushing is  $1.6 \pm 0.3$  N,<sup>39</sup> and the critical adhesion of the WPU-N2% coating with hydroxyapatite is much greater than the brush force of the toothbrush, indicating that the coating possesses a certain binding force with the teeth.

## 4 Conclusions

The novel nerol-segmented waterborne polyurethane nano-coating designed in this study can bind with calcium ions on the surface of tooth enamel, forming a protective layer that shields teeth from acid erosion in an acidic environment. The moderate addition of nerol can balance the hydrophilicity of the coating, improve the transparency and flatness, and endow the coating with anti-protein adhesion and anti-inflammatory properties. Dental erosion resulting from the consumption of carbonated beverages is a prevalent issue in daily life. In our study, uncoated and coated teeth were exposed to cola for 3 days. On the first day, uncoated teeth exhibited flaky staining, while none of the crown surfaces of coated teeth were stained. However, on the second day, the crown surfaces of the WPU-N4%- and WPU-N8%-coated groups showed spotty staining, indicating coating loss. This may be attributed to excessive nerol, which reduces coating hardness and carboxyl-group content. Additionally, the WPU-8% coating may also be associated with dissolution-induced loss. Overall, the WPU-N2% coating showed relatively good performance in all aspects, and thus has good prospects for application in the prevention of dental erosion.

## Conflicts of interest

There are no conflicts to declare.

## Acknowledgements

This research was financially supported by the Lishui City Public Welfare Technology Application Research Project (No. 2022GYX02) and Lishui University of Dentistry first-class discipline open subject fund.

## References

- 1 P. Kanzow, F. J. Wegehaupt, T. Attin, *et al.*, Etiology and pathogenesis of dental erosion, *Quintessence Int.*, 2016, **47**(4), 275–278.
- 2 N. Schlüter, T. Jäggi and A. Lussi, Is dental erosion really a problem?, *Adv. Dent. Res.*, 2012, **24**(2), 68–71.
- 3 F. Inchingolo, G. Dipalma, D. Azzollini, *et al.*, Advances in Preventive and Therapeutic Approaches for Dental Erosion: A Systematic Review, *Dent. J.*, 2023, **11**(12), 274.
- 4 J. Han, L. Kiss, H. Mei, *et al.*, Chemical aspects of human and environmental overload with fluorine, *Chem. Rev.*, 2021, **121**(8), 4678–4742.
- 5 L. K. Foong, M. M. Foroughi, A. F. Mirhosseini, *et al.*, Applications of nano-materials in diverse dentistry regimes, *RSC Adv.*, 2020, **10**(26), 15430–15460.
- 6 X. Mao, Z. Ye, J. Liang, J. Lin, X. Mei, D. Deng, R. Shi and Z. Wang, Copper Based metal organic framework/polymer foams with long-lasting antibacterial effect, *Iran. Polym. J.*, 2024, DOI: [10.1007/s13726-024-01314-9](https://doi.org/10.1007/s13726-024-01314-9).
- 7 M. F. Maitz, Applications of synthetic polymers in clinical medicine, *Biosurf. Biotribol.*, 2015, **1**(3), 161–176.
- 8 D. M. da Silva Ávila, R. F. Zanatta, T. Scaramucci, *et al.*, Influence of bioadhesive polymers on the protective effect of fluoride against erosion, *J. Dent.*, 2017, **56**, 45–52.
- 9 H. Honarkar, Waterborne polyurethanes: A review, *J. Dispersion Sci. Technol.*, 2018, **39**(4), 507–516.
- 10 L. Yin, B. Zhang, M. Tian, *et al.*, Synthesis and applications of bio-based waterborne polyurethane, a review, *Prog. Org. Coat.*, 2024, **186**, 108095.
- 11 X. Shi, S. Gao, C. Jin, *et al.*, A facile strategy to fabricate a lignin-based thermoset alternative to formaldehyde-based wood adhesives, *Green Chem.*, 2023, **25**(15), 5907–5915.
- 12 H. Wang, X. Shi, Y. Xie, *et al.*, A furan-containing biomimetic multiphase structure for strong and supertough sustainable adhesives, *Cell Rep. Phys. Sci.*, 2023, **4**(4), 101374.
- 13 J. Liu, X. Shi, L. Ma, *et al.*, Facile design of renewable lignin copolymers by photoinitiated RAFT polymerization as Pickering emulsion stabilizers, *Green Chem.*, 2023, **25**(14), 5428–5437.
- 14 R. Fukuda, Y. Yoshida, Y. Nakayama, *et al.*, Bonding efficacy of polyalkenoic acids to hydroxyapatite, enamel and dentin, *Biomaterials*, 2003, **24**(11), 1861–1867.
- 15 Q. Lan, X. Zhang, J. Liang, *et al.*, Multifunctional polyeugenol-based nanoparticles with antioxidant and antibacterial properties, *Particuology*, 2024, **87**, 194–204.
- 16 C. Jo, S. S. Kim, B. Rukmanikrishnan, *et al.*, Properties of Cellulose Pulp and Polyurethane Composite Films Fabricated with Curcumin by Using NMMO Ionic Liquid, *Gels*, 2022, **8**(4), 248.
- 17 B. M. Kim, J. S. Choi, S. Jang, *et al.*, Sustainable Strategies for Synthesizing Lignin-Incorporated Bio-Based Waterborne Polyurethane with Tunable Characteristics, *Polymers*, 2023, **15**(19), 3987.



18 Y. L. Uscátegui, L. E. Díaz, J. A. Gómez-Tejedor, *et al.*, Candidate polyurethanes based on castor oil (*ricinus communis*), with polycaprolactone diol and chitosan additions, for use in biomedical applications, *Molecules*, 2019, **24**(2), 237.

19 J. Xiang, S. Yang, J. Zhang, *et al.*, The preparation of sorbitol and its application in polyurethane: a review, *Polym. Bull.*, 2021, 1–18.

20 T. H. C. Marques, M. L. B. G. C. Branco and D. dos Santos Lima, Evaluation of the neuropharmacological properties of nerol in mice, *World J. Neurosci.*, 2013, **03**(1), 32–38.

21 S. Saalah, L. C. Abdullah, M. M. Aung, *et al.*, Waterborne polyurethane dispersions synthesized from jatropha oil, *Ind. Crops Prod.*, 2015, **64**, 194–200.

22 E. S. Negim, L. Bekbayeva, G. A. Mun, *et al.*, Effects of NCO/OH ratios on physico-mechanical properties of polyurethane dispersion, *World Appl. Sci. J.*, 2011, **14**(13), 402–407.

23 A. K. Das, K. Mitra, A. J. Conte, *et al.*, Lignin-A green material for antibacterial application—A review, *Int. J. Biol. Macromol.*, 2024, 129753.

24 H. Liang, L. Liu, J. Lu, *et al.*, Castor oil-based cationic waterborne polyurethane dispersions: Storage stability, thermo-physical properties and antibacterial properties, *Ind. Crops Prod.*, 2018, **117**, 169–178.

25 Q. Chen, X. Xu, X. Zhang, *et al.*, Valorization of isocyanates using castor oil-based protective strategies: Performance and comparison as waterborne adhesive additives, *Ind. Crops Prod.*, 2023, **195**, 116392.

26 M. C. Delpech and G. S. Miranda, Waterborne polyurethanes: influence of chain extender in ftir spectra profiles, *Cent. Eur. J. Eng.*, 2012, **2**, 231–238.

27 P. Fagundes, T. K. Carniel, M. C. Hall, *et al.*, Encapsulation of Nerol Oil in Polycaprolactone Polymer and Stability Evaluation, *J. Polym. Environ.*, 2022, **30**(1), 125–135.

28 A. Sukhanova, S. Bozrova, P. Sokolov, *et al.*, Dependence of nanoparticle toxicity on their physical and chemical properties, *Nanoscale Res. Lett.*, 2018, **13**, 1–21.

29 S. Saalah, L. C. Abdullah, M. M. Aung, *et al.*, Waterborne polyurethane dispersions synthesized from jatropha oil, *Ind. Crops Prod.*, 2015, **64**, 194–200.

30 W. H. De Jong, W. I. Hagens, P. Krystek, *et al.*, Particle size-dependent organ distribution of gold nanoparticles after intravenous administration, *Biomaterials*, 2008, **29**(12), 1912–1919.

31 C. Sell, *Chemistry of Essential oils[M]//Handbook of Essential Oils*, CRC Press, 2020, pp. 161–189.

32 F. Song, H. Koo and D. Ren, Effects of material properties on bacterial adhesion and biofilm formation, *J. Dent. Res.*, 2015, **94**(8), 1027–1034.

33 S. Türk, Characterization of chitosan/polyethylenimine film layer as a novel anti-fog coating surface, *J. Appl. Polym. Sci.*, 2022, **139**, e52884.

34 H. Sun, Ab initio characterizations of molecular structures, conformation energies, and hydrogen-bonding properties for polyurethane hard segments, *Macromolecules*, 1993, **26**(22), 5924–5936.

35 S. Hosseini, F. Ibrahim, I. Djordjevic, *et al.*, Polymethyl methacrylate-co-methacrylic acid coatings with controllable concentration of surface carboxyl groups: A novel approach in fabrication of polymeric platforms for potential bio-diagnostic devices, *Appl. Surf. Sci.*, 2014, **300**, 43–50.

36 U. Böhme and U. Scheler, Effective charge of bovine serum albumin determined by electrophoresis NMR, *Chem. Phys. Lett.*, 2007, **435**(4–6), 342–345.

37 H. Saari, S. Halinen, K. Ganlöv, *et al.*, Salivary mucous glycoprotein MG1 in Sjögren's syndrome, *Clin. Chim. Acta*, 1997, **259**(1–2), 83–96.

38 Y. Murase, H. Kotake, S. Kusakabe, *et al.*, Use of new scratch test and tensile test for evaluation of bond strength of self-adhesive flowable resin composite for repair of artificial tooth erosion, *Dent. Mater. J.*, 2020, **39**(3), 435–443.

39 H. Hayasaki, I. Saitoh, K. Nakakura-Ohshima, *et al.*, Tooth brushing for oral prophylaxis, *Jpn. Dent. Sci. Rev.*, 2014, **50**(3), 69–77.

